*Progress In Electromagnetics Research, PIER 88, 149–161, 2008*

# AN IMPROVEMENT OF THE GE-ESSELLE'S METHOD FOR THE EVALUATION OF THE GREEN'S FUNCTIONS IN THE SHIELDED MULTILAYERED STRUCTURES

**H. Li, H. G. Wang, and H. Zhang**

The Electromagnetics Academy at Zhejiang University
Zhejiang University
Hangzhou 310027, China

**Abstract**—In this paper, we improve the Ge-Esselle's (GE's) method and apply it to calculate the multilayered Green's functions in the shielded structures. In the improved GE's method, 1) the poles are first extracted using a recursive contour integration method; 2) then the general pencil-of-function (GPOF) is applied to approximate the part of the spectral-domain Green's functions (with the poles contributions being extracted) just along the real axis of the $k_\rho$ plane instead of the rooftop shaped path defined in the original GE's method; 3) Subsequently, an analytical identity is employed to obtain the spatial-domain Green's functions. In step 2), a smoothing procedure is also applied here to eliminate the abrupt peak of the sampled spectral-domain Green's function caused by the finite machine accuracy of the poles locations. The numerical results in this paper show that the improved GE's method can accurately and efficiently calculate the Green's functions in the shielded multilayered structure.

## 1. INTRODUCTION

In recent years, researchers have paid much attention to the multilayered structures encountered in the electromagnetic (EM) analysis of microstrip antennas and radio frequency integrated circuits (RFICs). In modeling the EM characteristics of these structures, we usually employ the method of moments (MoM), in which the accurate and efficient calculations of the multilayered Green's functions are very critical. The multilayered Green's functions are expressed in the forms of Sommerfeld integrals (SIs). However, the numerical evaluation of

SIs is time consuming since the integrands are both highly oscillating and slowly converging.

The discrete complex image method (DCIM), developed by Fang et al. [1], was proposed for efficient calculation of the spatial-domain multilayered Green's functions by expressing them using the complex image terms. This saves a lot of CPU time compared with the direct SIs. Based on this original idea of DCIM, researchers have suggested a lot of improvements to make it much more efficient and robust [2–5]. With these improvements, the DCIM does work in most conditions, but we found that it does not work well in the shielded structure, that is the first and the last interfaces are both perfect electric conductors (PECs), when $\rho$ (the horizontal distance between the source point and the field point) is larger than a certain value for the shielded multilayered structure.

A new complex image method based on a class of semi-infinite integrals of Bessel functions that have the closed-form solutions has been recently presented by Ge and Esselle [6]. The main characteristic is using an analytical expression [7, 8] to evaluate the spatial-domain Green's functions efficiently. Its precision is usually high and can tackle the situation mentioned above perfectly. However, because the contribution of surface-wave poles (SWPs) is always large, only performing the general pencil-of-function (GPOF) method [9] along the rooftop shaped path in the Ge-Esselles's (GE's) method cannot take into account the surface waves and guided waves contributions.

In this paper, we have some improvements to make the GE's method more robust and efficient for the shielded multilayered structure. They are listed below.

1) Extraction of SWPs using a recursive contour integration method [10].
2) Use a smoothing method to smooth the abrupt peak caused by the finite machine accuracy of the locations of poles. An interpolation technique that will be discussed later in Section 3.3 is applied to smooth the abrupt peaks.
3) The GPOF method is applied to approximate the remaining spectral-domain Green's functions along the path of the real axis of the $k_\rho$ plane instead of the rooftop shaped path suggested in the original GE's method. We will find benefits in the following examples.

To investigate the ranges of the applicability of the improved GE's method, here, we test two examples, i.e., a shielded 3-layer problem and a 5-layer medium without a shield at the top. We see that the improved GE's method proposed in this paper can accurately calculate

the shielded problem, while the DCIM method and the original GE's method do not work well. However, for the unshielded problem, the DCIM works well but the improved GE's method fails.

## 2. THE DIFFICULTY ENCOUNTERED BY THE DCIM FOR THE SHIELDED STRUCTURE

The basic idea of the DCIM is to approximate the spectral-domain Green's functions into series of exponentials using Prony or the GPOF method [2]. But we found that in a case the DCIM does not yield the results as expected. In the shielded structure, when the first and the last interfaces are both PECs, the values of spatial-domain Green's function $G_{xx}$ (the $x$ component of spatial-domain vector potential $\overrightarrow{A}$ created by the $x$-directed electric dipole) oscillate rapidly around the accurate values performed by the SIs.

We consider the same microstrip structure defined in [10], shown in Fig. 1(a). The source point and the field point are in the same layer, $z = z' = 0.254\,\text{mm}$. We used the two-level technique from [2]. Fig. 1(b) shows the integration path on the $k_z$ plane, where $T_{01}$ and $T_{02}$ are two parameters that determine the shape and length of the integration path. Fig. 1(c) shows the corresponding integration path (composed of $C_{ap1}$ and $C_{ap2}$) on the $k_\rho$ plane.

**Case 1:** $T_{01} = 600$, $T_{02} = 80$, the number of complex images is 16 and the samples on $C_{ap1}$ and $C_{ap2}$ both equal to 200. Fig. 2(a) shows the plots of $G_{xx}$ using the DCIM and the SIs and Fig. 2(b) shows the relative error of the DCIM (we set the values of the SIs as the reference). We can see that the error is unacceptable when $k_0\rho > 1$.

**Case 2:** $T_{01} = 600$, $T_{02} = 5$, the number of complex images is 16 and the samples on $C_{ap1}$ and $C_{ap2}$ both equal to 200. Fig. 3(a) shows the plots of $G_{xx}$ using the DCIM and the SIs and Fig. 3(b) shows the relative error of the DCIM. We can see that the error is too large when $k_0\rho > 2$.

**Case 3:** $T_{01} = 600$, $T_{02} = 5$, the number of complex images is 6 and the samples on $C_{ap1}$ and $C_{ap2}$ both equal to 200. Fig. 4(a) shows the plots of $G_{xx}$ using the DCIM and the SIs and Fig. 4(b) shows the relative error of the DCIM. We can see that the error is too large when $k_0\rho > 1$.

**Case 4:** $T_{01} = 600$, $T_{02} = 5$, the number of complex images is 60 and the samples on $C_{ap1}$ and $C_{ap2}$ both equal to 200. Fig. 5(a) shows the plots of $G_{xx}$ using the DCIM and the SIs and Fig. 5(b) shows

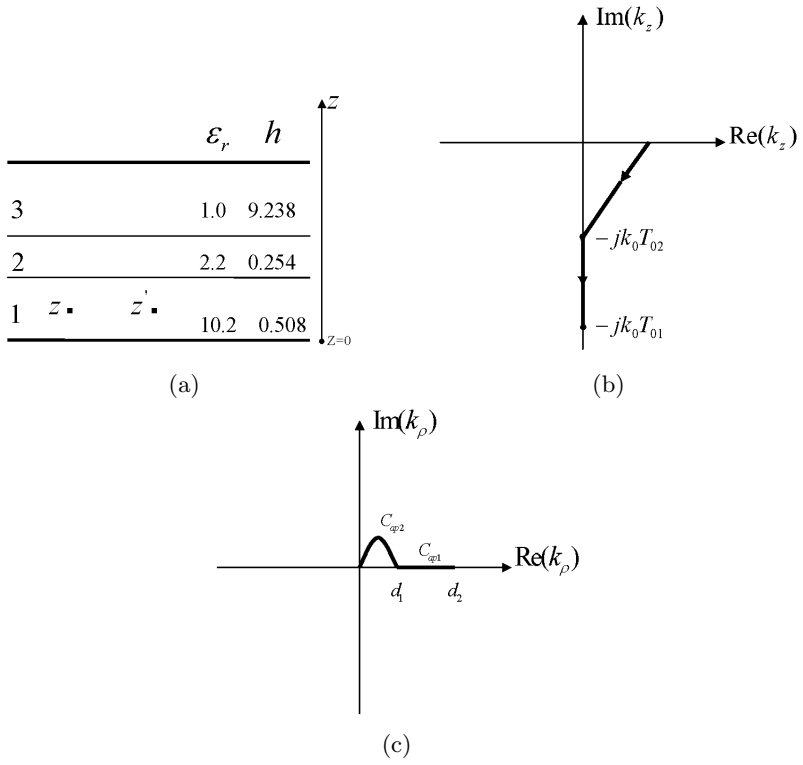


**Figure 1.** (a) The shielded structure, where the top interface and the bottom interface are both PECs. $z = z' = 0.254\,\text{mm}$. (b) The bold line is the path of performing the GPOF on the $k_z$ plane. (c) The corresponding path on the $k_\rho$ plane. $d_1 = \sqrt{T_{02}^2 + 1}k_0$, $d_2 = \sqrt{T_{01}^2 + 1}k_0$.

the relative error of the DCIM. We can see that the relative error can still be larger than 0.1.

From above, it is clear that with the reduction of $T_{02}$ and the increase of the number of complex images, the amplitude of the oscillation can be smaller, but not be eliminated.

For the shielded structure, there should be no branch point for the spectral-domain Green's functions on the finite region of the $k_\rho$ plane. However, when we perform the DCIM, we usually formulate the spectral-domain Green's functions in the form as formula (1) in

order to use the Sommerfeld identity conveniently.

$$\widetilde{G}(k_\rho) = \frac{F(k_\rho)}{2jk_{zi}} \tag{1}$$

where $k_{zi}^2 = k_i^2 - k_\rho^2$, $k_i$ is the wave number in the $i$th layer.

When $k_\rho = k_i$ (in the above cases, $k_i = 1337.792$), it would result in $k_{zi} = 0$. Thus there is an artificial "branch point", which does not physically exist. The first derivative of $F(k_\rho)$ at the location of the artificial "branch point" does not exist. We sample the values of spectral-domain Green's function $F(k_\rho)$ from the real axis of the $k_\rho$ plane using the method from [11], and also perform the DCIM along the same path. We can see from Fig. 6(a) that because of the existence of the artificial "branch point", the DCIM cannot accurately simulate

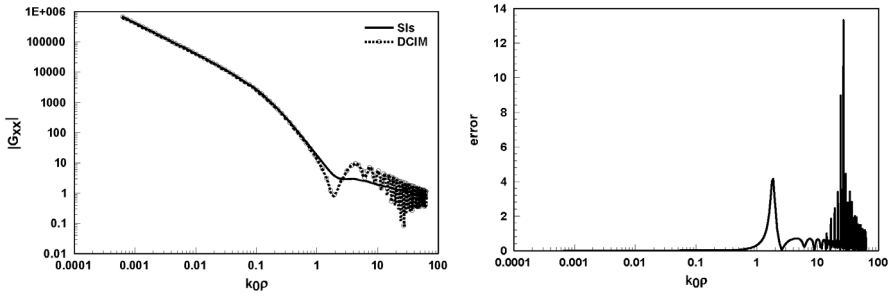


(a) (b)

**Figure 2.** (a) The spatial-domain Green's function $G_{xx}$ obtained by the DCIM and the SIs. (b) The relative error of the DCIM compared with the SIs.

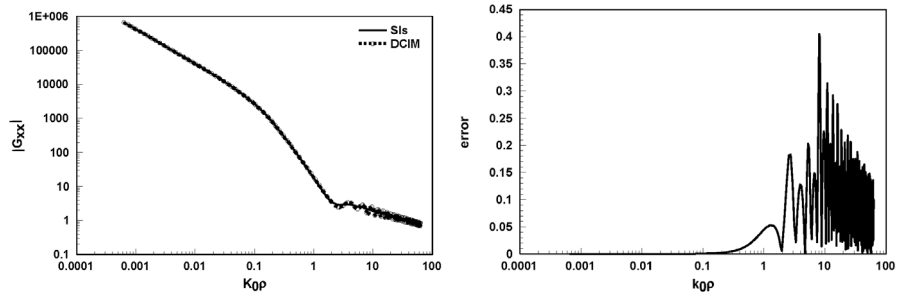


(a) (b)

**Figure 3.** (a) The spatial-domain Green's function $G_{xx}$ obtained by the DCIM and the SIs. (b) The relative error of the DCIM compared with the SIs.

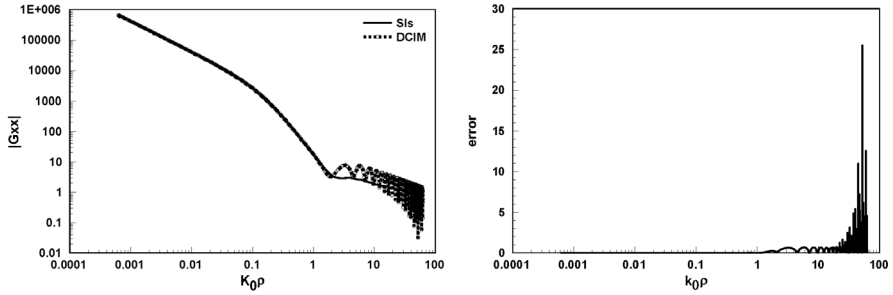


(a) (b)

**Figure 4.** (a) The spatial-domain Green's function $G_{xx}$ obtained by the DCIM and the SIs. (b) The relative error of the DCIM compared with the SIs.

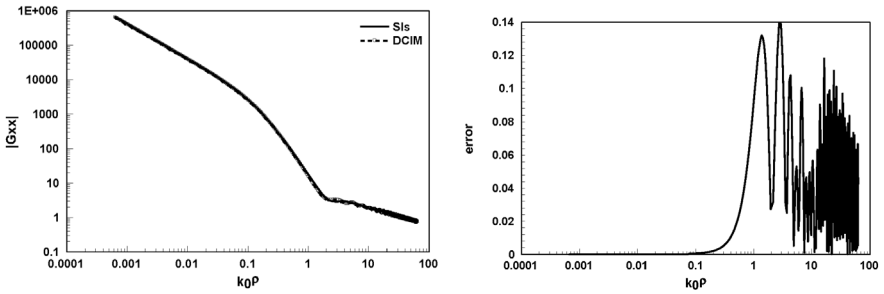


(a) (b)

**Figure 5.** (a) The spatial-domain Green's function $G_{xx}$ obtained by the DCIM and the SIs. (b) The relative error of the DCIM compared with the SIs.

the curve of the sampled values. Fig. 6(b) shows the detail of the sampled curve around the location of the "branch point".

## 3. THE IMPROVED GE'S METHOD

### 3.1. The Original GE's Method

We found the GE's method [6] does work for the mentioned case. The basic idea of this method is as follows:

1) Change the spectral-domain Green's function $\widetilde{G}(k_\rho)$ instead of $F(k_\rho)$ into series of exponentials (formula (2)) using the GPOF method along a rooftop shaped integration path $L_1$ (shown in Fig. 7) without extraction of SWPs and rewrite the SIs

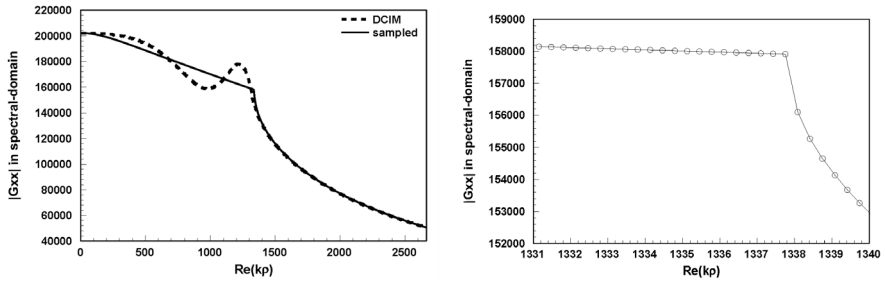


(a) (b)

**Figure 6.** (a) The values of the spectral-domain Green's function $\widetilde{G}_{xx}$ of the DCIM and the sampled one. (b) The detail information of the sampled spectral-domain Green's function when the real part of $k_\rho$ is in the interval 1331 to 1340.

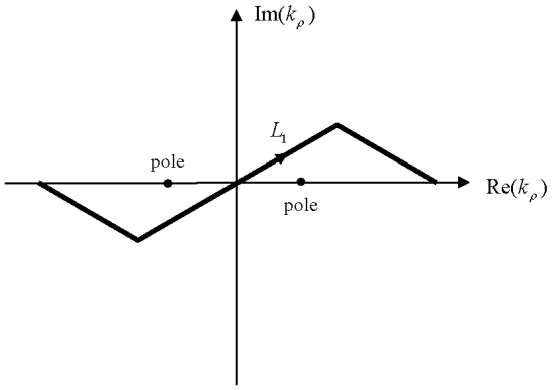


**Figure 7.** The suggested path in [6] while performing the GPOF.

(formula (3)) as

$$\widetilde{G}(k_\rho) = \sum_{i=1}^{M} b_i e^{-s_i k_\rho} \tag{2}$$

$$\int_0^\infty \widetilde{G}(k_\rho)\, J_0(k_\rho\rho) k_\rho dk_\rho = \sum_{i=1}^{M} b_i \int_0^\infty e^{-s_i k_\rho} J_0(k_\rho\rho) k_\rho dk_\rho. \tag{3}$$

2) Use an an analytical identity (formula (4)) to solve the integrations analytically [7, 8]

$$\int_0^\infty e^{-s_i\, k_\rho}\, J_0(k_\rho\rho) k_\rho\, dk_\rho = \frac{s_i}{\left(s_i^2 + \rho^2\right)^{3/2}}. \tag{4}$$

Here we briefly introduce the path suggested in [6], shown in Fig. 7. A two-level technique [2] is employed to perform the approximation, viz., a finite rooftop shaped integration path $L_1$ composed of two straight lines 1 and 2 is chosen. The two equations of the two straight lines are

$$L_1^1 : k_\rho = t + j\frac{t}{T_0}, \quad 0 \le t \le t_0 \tag{5}$$

$$L_1^2 : k_\rho = t + j\frac{(t_1 - t)t_0}{T_0(t_1 - t_0)}, \quad t_0 \le t \le t_1 \tag{6}$$

In this example, as suggested in [6], we set $T_0$ to be 10, $t_0$ to be $2k_1$ and $t_1$ to be $10k_1$, where $k_1 = \sqrt{10.2}k_0$.

However, if we apply the exact procedures from [6] to the example in Fig. 1(a), we found that the results are not as expected. Fig. 8 shows the plots of spatial-domain Green's function using the original GE's method and the SIs. We can see the error of the GE's method is unacceptable for the dynamic part. So we need to do some improvements.

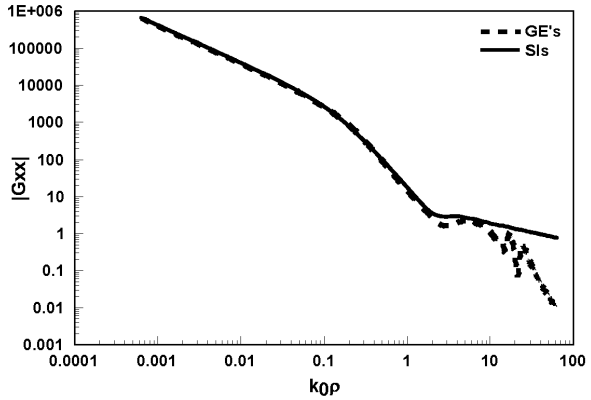


**Figure 8.** The magnitude of $G_{xx}$ using the GE's method and the SIs without the extraction of SWPs.

### 3.2. First Improvement: Extraction of the SWPs

As we know, the contribution of SWPs is always large. Thus, before adopting the GE's method, we need to extract the SWPs (formula (7)). After this, we perform the GPOF along the same integration path (shown in Fig. 7). The results are shown in Fig. 9. We can see that it is

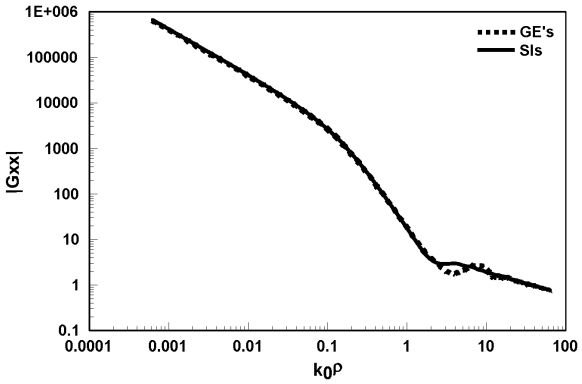


**Figure 9.** The magnitude of $G_{xx}$ using the GE's method and the SIs with the extraction of SWPs.

much better than the original method. This means that the procedure of the extraction of SWPs is necessary.

$$\widetilde{G}(k_\rho) = \widetilde{G} - \widetilde{G}_q - \widetilde{G}_s \tag{7}$$

where $\widetilde{G}_q$ and $\widetilde{G}_s$ stand for the contribution of quasi-static images and SWPs, respectively.

Here the procedure of extraction of the SWPs we used is adopted from [3, 12, 13]. To let readers clearly understand this, here we briefly introduce it as follows:

1) We confirm a rectangular region we are interested on the $k_\rho$ plane and construct a rectangle which is a little larger, so that it can contain the former rectangle completely.
2) Perform a contour integration along the four edges of the larger rectangle. If the result is zero, it indicates that there is no pole in this region. If not, there exist poles.
3) Divide the smaller rectangle into 4 equally rectangles and perform the above procedures recursively unless the rectangle containing poles shrinks into a much smaller one.
4) Apply Muller's method to solve the zeros of the reciprocal of the spectral-domain Green's function in the rectangle, that is the poles of the spectral-domain Green's function.
5) Use a check technique to make sure that every pole is counted only once. The basic idea is to check if the distance of two poles are less than a threshold value, i.e., $10^{-8}$. If so, we consider the two poles is actually the same one.

### 3.3. Second Improvement: A New Integration Path

We can see from Fig. 9 that though it is much better with the extraction of SWPs, there is still some variation when $1 < k_0\rho < 10$. Therefore we did another improvement, viz., after the extraction of SWPs, performed the GPOF along the real $k_\rho$ axis (shown in Fig. 10) instead of the rooftop shaped path in Fig. 7.

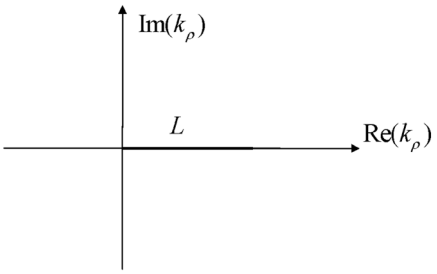


**Figure 10.** The integration path we suggested.

But we found another problem: the values of the spectral-domain Green's function $\widetilde{G}(k_\rho)$ are not smooth in some region or just at a point after the extraction of SWPs. Because of the finite machine precision, the locations of poles always have some errors compared with the true locations of poles. This could cause abrupt peaks around the poles when the spectral function $G(k_\rho)$ subtracts the contribution of SWPs. So we used a smoothing technique to smooth the sampled values on the real $k_\rho$ axis. The key procedures are listed as follows:

1) Locate a point P that is the nearest to the pole and start the following operations.
2) Obtain the forward differences of the spectral-domain Green's functions at the points on the left hand side of the point P.
3) For a point on the left hand side of P, check if the relative error of two near differences exceeds a small value, i.e., 0.01. If so, the variation of this point is judged to be very drastic and we name this point abnormal point. Otherwise we name it the normal point.
4) Using a similar manner, we can find the normal points on the right hand side. Use the values at the normal points on both sides which are the nearest to point P to interpolate the values of spectral-domain Green's function at those abnormal points, which are between these two normal points.

Figure 11(a) shows the spectral-domain Green's function before and after the smoothing technique (in this example, there is only one

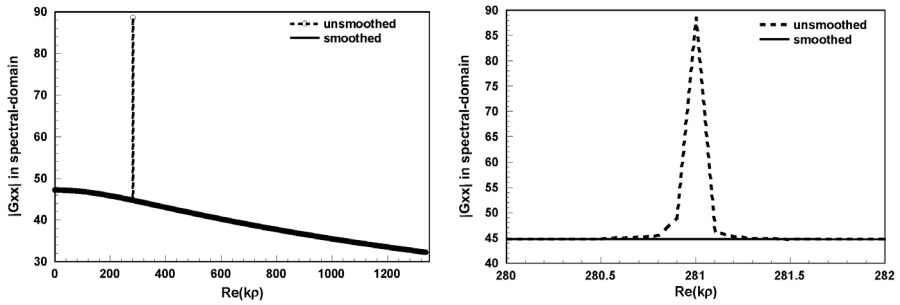


(a) (b)

**Figure 11.** (a) Before and after the smoothing procedure for the poles-extracted spectral-domain Green's function $\widetilde{G}_{xx}$. (b) The detail of the difference of before and after the smoothing procedure for real $k_\rho$ in the interval of 280 to 282.

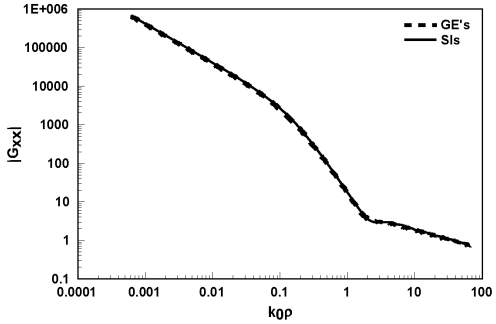


**Figure 12.** The coincidence of the improved GE's method and the SIs.

pole at $k_\rho = (280.976, -2.55177e-15)$). Fig. 11(b) shows the real $k_\rho$ in the interval between 280 and 282. After using the interpolation technique, the peak is eliminated.

After the above procedures, perform the GPOF along the real $k_\rho$ axis to approximate the remaining functions into series of exponentials. At last, an analytical identity is used. The results can be seen from Fig. 12. These two methods coincide with each other perfectly.

Recently, the problem of substrate integrated waveguide (SIW) has received a lot of attention [14]. According to the image method, this problem can be equivalent to the problem with infinite source points (including the real image source points) in the multilayered shielded structure as shown in Fig. 13. Obviously, the improved GEs method can be used to efficiently calculate the contribution to the field

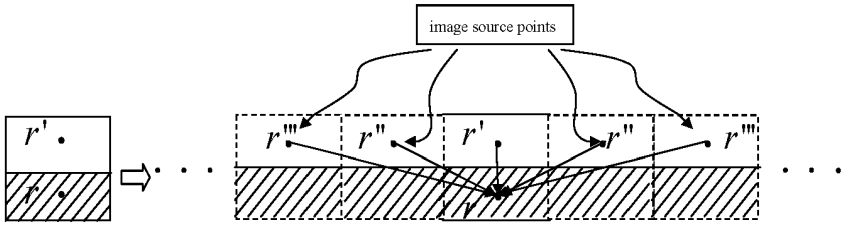


**Figure 13.** The magnitudes of the improved GE's method and the SIs in the unshielded structure.

point from each source point in the equivalent problem. Consequently, the superposition principle can be applied to sum these contributions up to form the Green's function value of the original problem. This will be our future work.

## 4. CONCLUSION

In this paper, some improvements are proposed to make the GE's method more robust and efficient. We extract SWPs before using the GPOF and perform the GPOF along the real $k_\rho$ axis. We also suggest a technique to smooth the sampled points. With these improvements, the GE's method can be used to efficiently calculate the multilayered Green's functions of the shielded stratified structure. The numerical examples given in this paper confirm this.

## ACKNOWLEDGMENT

This work was supported by National Nature Science Foundation of China No. 60501017.

## REFERENCES

1. Fang, D. G., J. J. Yang, and G. Y. Delisle, "Discrete image theory for horizontal electric dipoles in a multilayered medium," *IEE Proc.-H*, Vol. 135, 297–303, Oct. 1988.
2. Aksun, M. I., "A robust approach for the derivation of closed-form Green's functions," *IEEE Trans. Mircowave Theory Tech.*, Vol. 44, 651–658, May 1996.
3. Ling, F. and J. M. Jin, "Discrete complex image method for Green's functions of general multilayer media," *IEEE Trans. Microw. Guided Wave Lett.*, Vol. 10, 400–402, Oct. 2000.

4. Hu, B. and W. C. Chow, "Fast inhomogeneous plane wave algorithm for electromagnetic solution in layered medium structure-2D case," *Radio Sci.*, Vol. 35, 31–43, Jan.–Feb. 2000.
5. Abdelmagedd, A. K. and M. S. Ibranhim, "On enhancing the accuracy of evaluating Green's functions for multilayered media in the near-field region," *Progress In Electromagnetics Research M*, Vol. 2, 1–14, 2008.
6. Ge, Y. and K. P. Esselle, "New closed-form Green's functions for microstrip structure — Theory and results," *IEEE Trans. Antennas Propagat.*, Vol. 50, 1556–1560, June 2002.
7. Watson, G. N., *A Treatise on the Theory of Bessel Functions*, 2nd edition, Cambridge University Press, Cambridge, 1944.
8. Gradsbteyn. I. S. and L. M. Ryzbik, *Table of Integrals, Series, and Products*, 6th edition, Academic Press, 2000.
9. Hua, Y. and T. K. Sarkar, "Generalized pencil-of-function method for extracting poles of an EM system from its transient response," *IEEE Trans. Antennas Propagat.*, Vol. 37, 229–234, Feb. 1989.
10. Ling, F., J. Liu, and J. M. Jin, "Efficient electromagnetic modeling of three-dimensional multilayer microstrip antennas and circuits," *IEEE Trans. Mircowave Theory Tech.*, Vol. 50, 1628–1635, June 2002.
11. Michalski, K. A. and D. Zheng, "Electromagnetic scattering and radiation by surfaces of arbitrary shape in layered media, part I: Theory," *IEEE Trans. Antennas Propagat.*, Vol. 38, 335–344, Mar. 1990.
12. Zhuang, L., W. Hu, W. Yu, G.-Q. Zhu, and Y. H. Zhang, "Automatic incorporation of surface wave poles in discrete complex image method," *Progress In Electromagnetics Research*, PIER 80, 161–178, 2008.
13. Abdelmageed, A. K., "A new approach to evaluate the surface waves term for the nonsymmetrical components of Green's functions in multilayered media," *Progress In Electromagnetics Research M*, Vol. 4, 105–116, 2008.
14. Fang, D. G., F. Ling, and Y. Long, "Rectangular waveguide Green's function involving complex images," *IEEE AP-S Digest*, Vol. 2, 1045–1048, Newport Beach, June 1995.